

# A multiply convergent platform for the synthesis of trioxacarcins

Jakub Švenda, Nicholas Hill, and Andrew G. Myers<sup>1</sup>

Department of Chemistry and Chemical Biology, Harvard University, 12 Oxford Street, Cambridge, MA 02138

Edited by Stuart L. Schreiber, Broad Institute, Cambridge, MA, and approved November 29, 2010 (received for review October 15, 2010)

Many first-line cancer drugs are natural products or are derived from them by chemical modification. The trioxacarcins are an emerging class of molecules of microbial origin with potent antiproliferative effects, which may derive from their ability to covalently modify duplex DNA. All trioxacarcins appear to be derivatives of a nonglycosylated natural product known as DC-45-A2. To explore the potential of the trioxacarcins for the development of small-molecule drugs and probes, we have designed a synthetic strategy toward the trioxacarcin scaffold that enables access to both the natural trioxacarcins and nonnatural structural variants. Here, we report a synthetic route to DC-45-A2 from a differentially protected precursor, which in turn is assembled in just six steps from three components of similar structural complexity. The brevity of the sequence arises from strict adherence to a plan in which strategic bond-pair constructions are staged at or near the end of the synthetic route.

chemical synthesis | DNA alkylation | anticancer

The trioxacarcins are highly concatenated, densely oxygenated molecules encoded within the genes of various streptomycetes and potently inhibit the growth of cultured human cancer cell lines (1–4). Approximately 20 individual trioxacarcins have been structurally characterized; all appear to be built upon or closely related to the natural product DC-45-A2 (1) (5). The diversity of the trioxacarcin class is well represented by the four compounds that are depicted in Fig. 1 alongside the anthracycline antibiotic daunomycin (daunorubicin, long used in chemotherapy for acute myelogenous leukemias) and nogalamycin, presented in a manner that emphasizes their structural similarities. The trioxacarcins, however, have unique glycosylation patterns, contain a distinct linear aromatic core, and bear as their most distinguishing feature a highly unusual condensed polycyclic trisketal containing a spiro-epoxide. The latter is implicated to be key to the observed antiproliferative effects of the trioxacarcins, for it has been shown to serve as the point of covalent attachment of trioxacarcin A (6–8), the most potent family member in clonogenic assays (4) (with subnanomolar IC<sub>70</sub> values), to G residues of duplex DNA. An X-ray crystallographic analysis of a 2:1 complex of trioxacarcin A and an 8-mer duplex DNA oligonucleotide (8) reveals that the structure has features related to the (2:1) nogalamycin-DNA complex (9), with the linear aromatic cores of both small molecules bound intercalatively through the base stack and sugar residues positioned in the major and minor grooves, but unlike nogalamycin, trioxacarcin A covalently modifies the DNA duplex, by reaction of the spiro-epoxide with N7 of a flanking G residue as nucleophile (8). Other structurally distinct natural product families appear to function by pathways that may be mechanistically related (10, 11).

To realize their full potential as chemotherapeutic agents and to enable a broader study of the trioxacarcin class of DNA-binding molecules, we sought to develop a synthetic route that would allow for the preparation of a wide array of new trioxacarcins in amounts sufficient for biological evaluation. Toward this end and as a strategic objective, we determined to develop a route that approached maximal convergence, with the further specification that it be optimized toward bond-pair constructions between components

of similar complexity at or near the final step of the sequence. Although the importance of convergence in synthesis has long been appreciated (12–21), highly condensed polycyclic targets such as the trioxacarcins frequently do not lend themselves to convergent simplification of the type specified, and synthesis plans that might meet this objective can be stereochemically ambiguous and (partly as a consequence) may offer modest probability of success. As an important counterpoint, however, the end value of a route that successfully achieves a high degree of convergence by bond-pair constructions between components of similar complexity is made evident by the rapidity with which large numbers of structural analogs can be prepared and by the diversity of compounds that can be synthesized through variation of the coupling partners (21–23).

To address natural and nonnatural trioxacarcins broadly, we targeted for synthesis compound 2 and as its precursor the cyclic siloxane 3, differentially and orthogonally hydroxyl-protected derivatives of DC-45-A2 (1). By the retrosynthetic derivation outlined in Fig. 2, we envisioned that target 3 could be assembled in one step by a 1,3-dipolar cycloaddition reaction between the carbonyl ylide intermediate 4 and the aromatic aldehyde 5 (24, 25). Four diastereomeric cycloadducts can arise from the pairwise combinations of the two diastereofaces of reactants 4 and 5 (Fig. S1); only one (an *endo*-cycloadduct) is stereochemically congruent with natural trioxacarcins. Although each of the >20 prior examples of 1,3-dipolar cycloaddition reactions between a five-membered cyclic carbonyl ylide and an aromatic aldehyde was shown to proceed with *exo* selectivity (25, 26), we anticipated that different stereochemical outcomes might be achieved in the proposed cycloaddition reaction by variation of catalyst (both catalyzed and noncatalyzed carbonyl ylide–aldehyde cycloadditions are known) and/or substrate (such as by modification of the protective groups of the aldehyde component). We imagined that the carbonyl ylide intermediate 4 would derive in one step from the epoxy diazo diketone precursor 6, and that the aromatic aldehyde coupling component 5 could be assembled in a second convergent bond-pair construction, by base-promoted cyclization of the cyanophthalide 7 with the substituted cyclohexenone 8. The three precursors 6, 7, and 8 were viewed to be components of similar synthetic complexity, as determined by analysis of the number of steps required for their preparation.

## Results and Discussion

The densely functionalized epoxy diazo diketone 6, the precursor to the carbonyl ylide intermediate 4, was synthesized in eight steps, as shown in Fig. 3 *Left*, beginning with a highly diastereoselective

Author contributions: J.Š., N.H., and A.G.M. designed research; J.Š. and N.H. performed research; and J.Š., N.H., and A.G.M. wrote the paper.

The authors declare no conflict of interest.

This article is a PNAS Direct Submission.

Data deposition: The crystallography, atomic coordinates, and structural factors have been deposited in the Cambridge Structural Database, Cambridge Crystallographic Data Centre, Cambridge CB2 1EZ, United Kingdom (accession no. CCDC 788988).

<sup>1</sup>To whom correspondence should be addressed. E-mail: myers@chemistry.harvard.edu.

This article contains supporting information online at [www.pnas.org/lookup/suppl/doi:10.1073/pnas.1015257108/-DCSupplemental](http://www.pnas.org/lookup/suppl/doi:10.1073/pnas.1015257108/-DCSupplemental).

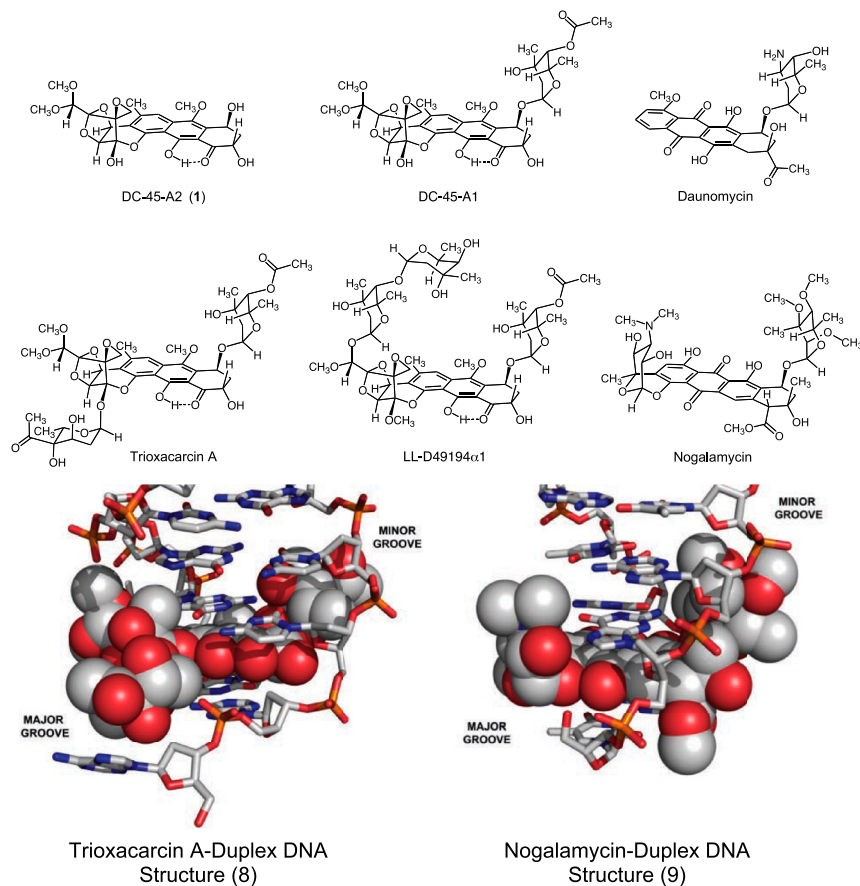


Fig. 1. Representative trioxacarcins and the anthracycline antibiotics daunomycin and nogalamycin.

auxiliary-controlled Baylis–Hillman reaction between the Oppolzer sultam-derived acrylimide **9** (1 eq) and anhydrous 2,2-dimethoxyacetaldehyde (3.0 eq) using 1,4-diazabicyclo[2.2.2]octane (DABCO, 0.3 eq) as catalyst in dichloromethane at 23 °C (16 h). The product of the reaction had incorporated two molecules of 2,2-dimethoxyacetaldehyde, and had expelled the sultam auxiliary by internal lactonization, as anticipated based on precedent (27). Methanolysis of the resulting lactone (triethylamine in methanol, 30 min, 23 °C) afforded the corresponding methyl ester (see *SI Appendix*), shown to be  $\geq 98\%$  enantiomerically pure by capillary GC analysis. Hydroxyl protection with *tert*-butyldimethylsilyl trifluoromethanesulfonate (1.2 eq) and *N,N*-diisopropylethylamine (1.5 eq) then afforded the *tert*-butyldimethylsilyl ether **10** (48% over three steps). Nucleophilic epoxidation of **10** at 0 °C (4.5 h) in the presence of *tert*-butylhydroperoxide (2.0 eq) and potassium *tert*-butoxide (0.1 eq) provided selectively the *anti*-epoxy ester **11** in 81% yield (*anti:syn* = 13:1) (28). Saponification of ester **11** (THF–MeOH–H<sub>2</sub>O, LiOH, 0 °C) and activation of the resulting carboxylic acid by treatment with isobutylchloroformate (1.05 eq) in the presence of Et<sub>3</sub>N (1.1 eq) at –20 °C with gradual warming to –10 °C followed by addition of a solution of diazomethane in ether (~0.25 M, 2.0 eq) and further warming to 23 °C provided, after chromatographic purification on triethylamine-deactivated silica gel, the epoxy diazo ketone **12** as a yellow oil (74% yield, two steps). Exposure of this product to triethylamine-trihydrofluoride in acetonitrile led to efficient cleavage of the *tert*-butyldimethylsilyl protective group, affording the corresponding secondary alcohol in nearly quantitative yield. Oxidation with Dess–Martin periodinane (1.1 eq) buffered with sodium bicarbonate then afforded the corresponding epoxy diazo dike-

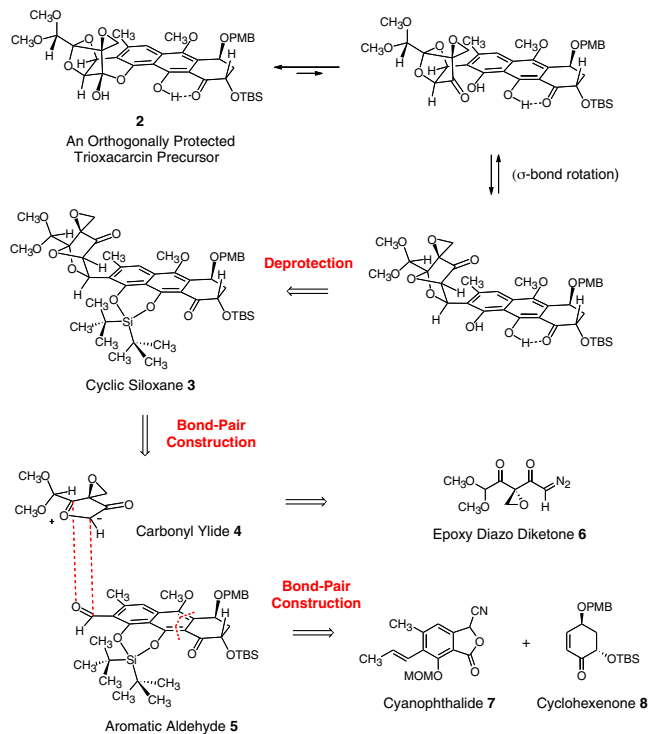


Fig. 2. Target identification and retrosynthetic analysis.

tone **6** as a light yellow oil in 77% yield (two steps). The epoxy diazo diketone **6** can be stored for several months without decomposition at  $-25^{\circ}\text{C}$  with care to exclude light.

The cyanophthalide **7** in 77% yield by brief exposure to cyanotrimethylsilane followed by extended treatment with glacial acetic acid (30, 31).

Two different routes were developed for the synthesis of the cyclohexenone fragment **8**. The preferred route, shown in Fig. 3 Right (see *SI Appendix* for an alternate route), employed L-malic acid as starting material and proceeded through a known four-step sequence to the lactone **17**. The latter product was transformed into the aldehyde **18** in 70% yield (two steps) by Weinreb amide formation (32) followed by oxidation with aqueous sodium hypochlorite (1.0 eq) in the presence of 2,2,6,6-tetramethylpiperidine-1-oxyl (TEMPO, 0.01 eq) and potassium

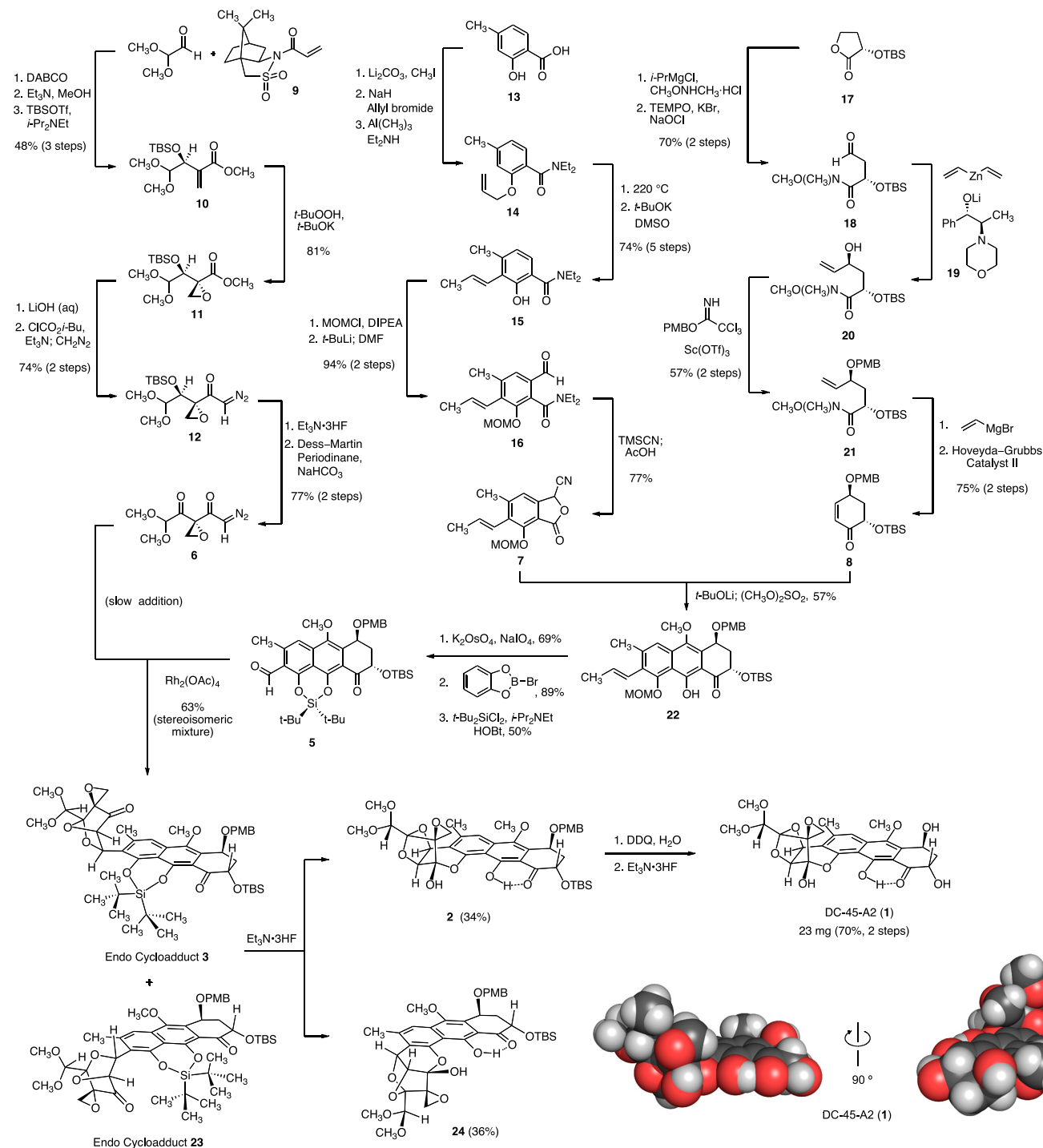


Fig. 3. A multiply convergent route for the synthesis of trioxacarcins.

bromide (0.1 eq). Addition of aldehyde **18** to a 1:1 mixture of divinylzinc (2.0 eq) and the amino alkoxide ligand **19** (2.0 eq) at  $-70^{\circ}\text{C}$  provided the 4*S*-alcohol **20** selectively (diastereomeric ratio 12:1), by which we infer that the substrate had reacted via bidendate coordination to the organometallic reagent (**33**). The product was susceptible to lactonization and so was protected immediately as the 4-methoxybenzyl ether (**21**) using 4-methoxybenzyl trichloroacetimidate (2.0 eq) and  $\text{Sc}(\text{OTf})_3$  as catalyst (0.03 eq, 57% yield over two steps, 12:1 mixture of C4 diastereomers, 17.8-g scale). Addition of vinylmagnesium bromide (3.0 eq) to amide **21** provided the divinyl ketone, which underwent smooth ring-closing metathesis in the presence of the second-generation Hoveyda–Grubbs ruthenium alkylidene catalyst (**34**) at  $55^{\circ}\text{C}$ , affording the diastereomerically pure cyclohexenone coupling component **8** in 75% yield after chromatographic purification.

In the first of two late-stage ring-forming (bond-pair) coupling reactions, components **7** and **8** were combined in a Kraus–Sugimoto cyanophthalide annulation reaction (**35**). Thus, addition of a solution of enone **8** (1 eq) to a cold solution of the cyanophthalide anion obtained by deprotonation of **7** (1.0 eq) with lithium *tert*-butoxide (3.0 eq) in tetrahydrofuran at  $-78^{\circ}\text{C}$  led to rapid formation of Michael addition product(s) (based on TLC analysis, not characterized); upon warming to  $-40^{\circ}\text{C}$  these underwent cyclization to form a single dihydroquinone phenolate, which was trapped in situ by monomethylation with dimethylsulfate ( $-26 \rightarrow 23^{\circ}\text{C}$ ). The anthrone methyl ether **22** was obtained in 57% yield (3-g scale, yellow foam) after chromatographic isolation, a process facilitated by the long-wavelength UV absorption of the product, with blue-green fluorescence, a characteristic of the trioxacarcins. Oxidative cleavage of the alkenyl side chain at  $0^{\circ}\text{C}$  ( $\text{NaIO}_4$ ,  $\text{K}_2\text{OsO}_4 \cdot 2\text{H}_2\text{O}$ , 2,6-lutidine) (**36**) then provided the corresponding aldehyde as an orange foam (69% yield). The methoxymethyl (MOM) protective group was selectively removed upon treatment of the latter product with *B*-bromocatecholborane (2.0 eq), affording an air-sensitive bisphenol intermediate (89% yield) as a yellow foam. Silylation (*t*- $\text{Bu}_2\text{SiCl}_2$ , HOBt, DIPEA,  $55^{\circ}\text{C}$ ) (**37**) then provided the much more stable di-*tert*-butylsiloxane derivative **5** (50% yield), the substrate for final coupling.

The fully oxygenated polycyclic skeleton of the trioxacarcins was assembled in one step by slow addition (syringe pump, 2 h) of a solution of the epoxy diazo diketone **6** (3.0 eq, 2.26 M in dichloromethane) to a stirring suspension of aldehyde **5** (1 eq, 0.75 M in dichloromethane), rhodium(II) acetate (0.05 eq), and powdered, activated 4 Å molecular sieves at  $23^{\circ}\text{C}$ . After filtration to remove the rhodium catalyst, the filtrate was concentrated, and the residue was purified by RP-HPLC to provide in 63% yield a mixture of diastereomeric cycloadducts in which the two *endo*-diastereomers (**3** and **23**) greatly predominated (Fig. 3 and *SI Appendix*). Pure samples of the individual diastereomers were obtained for spectroscopic analysis (see *SI Appendix*), but for preparative purposes it proved to be much more practical to separate the diastereomers after cleavage of the cyclic di-*tert*-butylsiloxane protective group (triethylamine-trihydrofluoride,  $23^{\circ}\text{C}$ , 15 min), where the *endo*-diastereomers alone underwent spontaneous hemiketalization; these products, both obtained as bright yellow oils, were easily separated by RP-HPLC [**24**, 52 mg (36% yield) and **2**, 48 mg (34% yield)]. Variation of the catalyst was indeed found to greatly influence the stereochemical outcome of the cycloaddition. For example, cycloaddition of **5** and **6** in the presence of copper(I) tetrakis(acetonitrile) afforded as the major product an *exo*-diastereomer (46%) that represented only 14% of the diastereomeric product distribution when rhodium(II) acetate was used as catalyst. Although we believe it likely that the efficiency and stereoselectivity of formation of the desired *endo*-cycloadduct (**3**) may be improved by further exploration of different catalysts, in its present form the rhodium(II) acetate-catalyzed transformation provides more than

sufficient quantities of material for biological evaluation and mechanistic study. Two-step deprotection of *endo*-hemiketal **2** (DDQ; triethylamine-trihydrofluoride) afforded synthetic DC-45-A2 (**1**) as a bright yellow powder (23 mg, 70% yield). Spectroscopic data for the synthetic substance were fully consistent with those reported for the natural product (**5**). Crystallization of synthetic DC-45-A2 from ethyl acetate-hexanes provided a single crystal suitable for X-ray diffraction analysis; two representations of the three-dimensional structure obtained are depicted in Fig. 3. This structure conforms fully with that proposed for the natural product (**5**) and shows that the spiro-epoxide is ideally aligned for opening by a G residue stacked upon the  $\pi$ -face of the tricyclic core. It is revealing that similar two-step deprotection of the stereoisomeric *endo*-hemiketal **24** (with the more electrophilic carbon of the spiro-epoxide oriented away from the tricyclic aromatic core) gave rise to a chlorohydrin derivative (25%), presumably arising from ring-opening of the spiro-epoxide by chloride ion during workup, as well as the expected spiro-epoxide, iso-DC-45-A2 (**25**, 22%, depicted in Fig. 4*A*). No such opening was observed with DC-45-A2. In contrast, in experiments evaluating the reactions of DC-45-A2 (**1**) and iso-DC-45-A2 with the G residue of a known DNA substrate for alkylation by trioxacarcin A (**7**), iso-DC-45-A2 was found to be unreactive, whereas **1** readily alkylated the DNA duplex, as discussed below.

We measured  $\text{IC}_{50}$  values of DC-45-A2, iso-DC-45-A2, and a fully synthetic analog, dideoxy-DC-45-A2 (**26**), which we prepared by the six-step route outlined in Fig. 3 without variation, save for the use of 2-cyclohexen-1-one as starting material in place of the substituted cyclohexenone coupling component **8**, in HeLa and H460 cell lines (Fig. 4*A*). DC-45-A2 inhibited the growth of both cell lines at micromolar concentrations. Dideoxy-DC-45-A2 was found to be a more potent growth inhibitor, with submicromolar  $\text{IC}_{50}$  values, and iso-DC-45-A2 was found to be inactive. Both DC-45-A2 and dideoxy-DC-45-A2 were found to modify a self-complementary 12-mer duplex oligonucleotide containing a single (central) G residue (**7**) at  $23^{\circ}\text{C}$ , as determined by nondenaturing polyacrylamide gel electrophoresis with in-gel fluorescence detection as well as liquid chromatography–mass spectrometry (LC-MS) experiments, albeit with different rates and efficiencies of alkylation (Fig. 4*B–D*). Although alkylation of the DNA duplex by DC-45-A2 proceeds with a half-life of hours at  $23^{\circ}\text{C}$ , the dideoxy-analog reacts with the DNA duplex within minutes at  $23^{\circ}\text{C}$  and with apparently greater efficiency (Fig. 4*C* and *D*). Iso-DC-45-A2 was not observed to modify the same DNA duplex under any conditions examined.

Heretofore, antiproliferative effects of nonglycosylated trioxacarcins such as DC-45-A2 have not been reported, so far as we are aware, nor has their chemistry with deoxyribonucleic acids been studied. Our findings suggest that the nonglycosylated, rigid polycyclic framework of DC-45-A2, with a naturally configured spiro-epoxide function, comprises structural features necessary and sufficient to provide an electrophile capable of alkylating G residues of duplex DNA, and that substantial variation in the rate, efficiency, and perhaps sequence specificity of DNA alkylation (not evaluated here) might be achieved by substitution upon this framework, which need not necessarily involve glycosylation. Structural variations by the convergent route reported can be achieved in two distinct ways, which together should allow for multiplicative enhancement of the pool of synthetic trioxacarcins. First, selective derivatization of the hydroxyl groups should be feasible by virtue of their orthogonal protection. Second, more deep-seated structural changes can be achieved by variation of any of the three coupling components [exemplified by the synthesis of dideoxy-DC-45-A2 (**26**) above]. We believe that the route to trioxacarcins described enables a comprehensive and broad evaluation of trioxacarcin-based structures as potential chemotherapeutic agents and provides a viable basis for their pro-

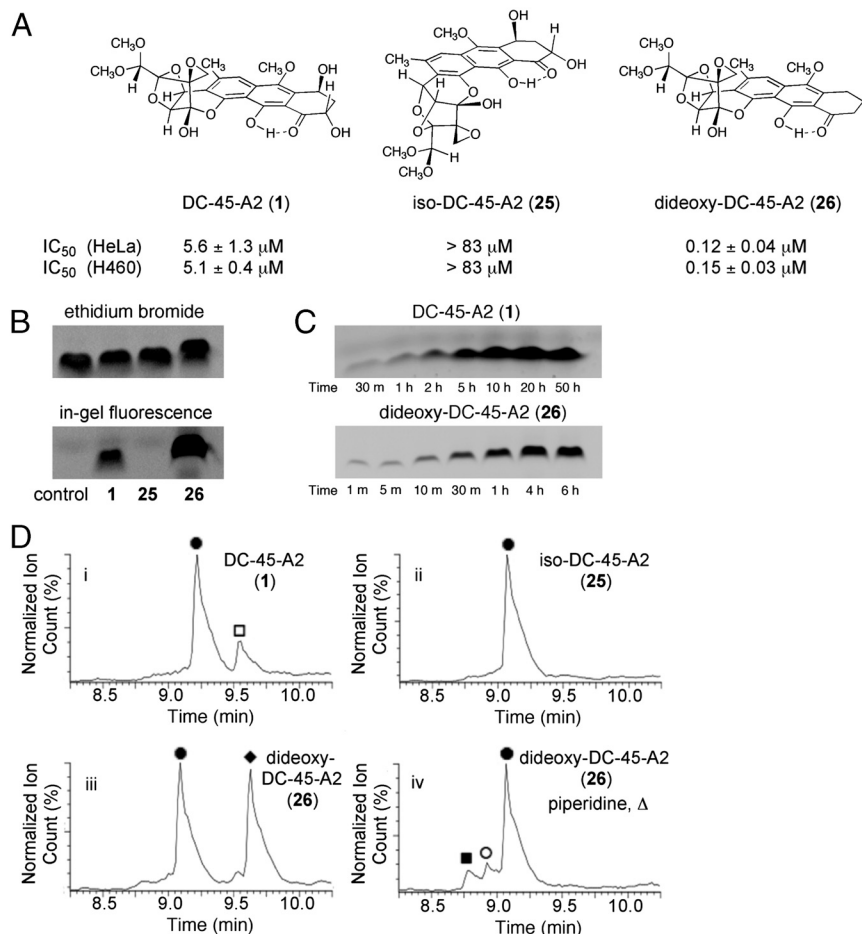


**Fig. 4.** Synthetic nonglycosylated trioxacarins, their antiproliferative activities in cultured human cancer cells, and DNA-modifying effects. (A) IC<sub>50</sub> values for DC-45-A2, iso-DC-45-A2, and dideoxy-DC-45-A2 measured in HeLa (cervical cancer) and H460 (lung cancer) cells lines. (B) Images of TBE 20% polyacrylamide gels of the products of the reaction of the self-complementary duplex 12-mer d(AATTACGTAATT) (100 μM) with DC-45-A2 (lane 2, 100 μM), iso-DC-45-A2 (lane 3, 100 μM), or dideoxy-DC-45-A2 (lane 4, 100 μM) for 2 h at 23 °C; visualized with ethidium bromide and by in-gel fluorescence. (C) Images of TBE gels of the products of the reaction of the self-complementary duplex 12-mer d(AATTACGTAATT) (100 μM) with DC-45-A2 or dideoxy-DC-45-A2 (25 μM) at 23 °C for the indicated times; visualized by in-gel fluorescence. (D) LC-MS chromatograms of reaction mixtures of the self-complementary duplex 12-mer d(AATTACGTAATT) (100 μM) and (i) DC-45-A2 (100 μM), (ii) iso-DC-45-A2 (100 μM), or (iii) dideoxy-DC-45-A2 (100 μM) after 24 h at 23 °C; iv depicts the LC-MS chromatogram of the reaction mixture of the self-complementary duplex 12-mer d(AATTACGTAATT) (100 μM) and dideoxy-DC-45-A2 (100 μM) after 24 h at 23 °C followed by the addition of piperidine (1 M) and heating for 30 min at 95 °C; ●, (AATTACGTAATT); □, (AATTACGTAATT • 1); ◆, (AATTACGTAATT • 26); ■, (pTAATT); ○ = (AATTACp).

duction on scales necessary to support clinical evaluation should preclinical studies support such advancement.

## Materials and Methods

**General.** Experimental procedures and spectral data for all compounds created for this study can be found in the *SI Appendix*. The experimental details, geometric parameters, perspective views, and three-dimensional supramolecular architecture associated with the X-ray crystal structure of DC-45-A2 are provided in *Tables S1–S3* and *Figs. S2* and *S3* of the *SI Appendix*.

**Preparation of DC-45-A2 (1).** 2,3-Dichloro-5,6-dicyanobenzoquinone (17.4 mg, 76.7 μmol, 1.2 eq) was added to a vigorously stirring, biphasic solution of differentially protected DC-45-A2 (2) (48 mg, 63.8 μmol, 1 eq) in dichloromethane (1.3 mL) and water (130 μL) at 23 °C. The reaction flask was covered with aluminum foil to exclude light. Over the course of 5 h, the reaction mixture was observed to change from myrtle green to lemon yellow. The product solution was partitioned between saturated aqueous sodium chloride solution (5 mL) and dichloromethane (50 mL). The layers were separated. The organic layer was dried over sodium sulfate. The dried solution

was filtered, and the filtrate was concentrated. The residue (1 eq, see above) was dissolved in acetonitrile (1.3 mL), and triethylamine-trihydrofluoride (208 μL, 1.28 mmol, 20 eq) was added at 23 °C. The reaction flask was covered with aluminum foil to exclude light. After 13.5 h, the reaction mixture was partitioned between saturated aqueous sodium chloride solution (10 mL) and dichloromethane (50 mL). The layers were separated. The organic layer was dried over sodium sulfate. The dried solution was filtered, and the filtrate was concentrated. The residue was purified by preparatory HPLC to provide 23 mg of the product, DC-45-A2 (1), as a bright yellow powder (70%).

**ACKNOWLEDGMENTS.** J.S. acknowledges Dr. Alfred Bader for his creation and generous financial support of the Alfred Bader Fellowship Program in Chemistry at Harvard University. Dr. Robert Yu measured the IC<sub>50</sub> values of DC-45-A2, iso-DC-45-A2, and dideoxy-DC-45-A2, which we acknowledge with appreciation. We thank Dr. Shao-Liang Zheng for his help with X-ray data collection and structure determination. Financial support from the National Institutes of Health (Grant CA047148) and the National Science Foundation (Grant CHE-0749566) is gratefully acknowledged.

1. Tomita F, Tamaoki T, Morimoto M, Fujimoto K (1981) Trioxacarins, novel antitumor antibiotics I. Producing organism, fermentation and biological activities. *J Antibiot* 34:1519–1524.

2. Tamaoki T, Shirahata K, Iida T, Tomita F (1981) Trioxacarins, novel antitumor antibiotics II. Isolation, physico-chemical properties and mode of action. *J Antibiot* 34:1525–1530.

